Dynamic pressure fluctuations at real-life plunge pool bottoms

E.F.R. Bollaert, P.A. Manso & A.J. Schleiss
Laboratory of Hydraulic Constructions of the Swiss Federal Institute of Technology Lausanne (EPFL), Switzerland

ABSTRACT: Scour of rock downstream of dam spillways may be generated by jet impact. Generally, jets impact into a plunge pool downstream and diffuse through the pool. This results in a turbulent shear layer, which generates significant pressure fluctuations that might enter underlying rock joints. Recent research performed at the Laboratory of Hydraulic Constructions in Lausanne revealed that these pressure fluctuations may be amplified inside rock joints and are directly responsible for progressive break-up of the rock. Hence, appropriate assessment of these pressure fluctuations is crucial for a physically correct scour evaluation. At present, a respective amount of data is available on pressure fluctuations measured on laboratory models and for perfectly flat pool bottoms. However, real-life plunge pools are characterized by a much more complicated bottom profile, which changes during scour formation. Therefore, a research project focuses on measurements of pressure fluctuations at appropriately shaped, laboratory scaled pool bottoms. The profiles to be tested have been derived from observed model and/or prototype cases. The obtained results are described in a companion paper.

1 INTRODUCTION

Scour of rock downstream of dam spillways is generated by high velocity jet impact. Generally, the falling jet impacts into a plunge pool downstream of the dam and diffuses through the water depth of the pool. This results in a highly turbulent and aerated shear layer at the water-rock interface. This shear layer is constituted of turbulent eddies, which generate significant dynamic pressure fluctuations that might enter underlying rock joints. Recent experimental and numerical research performed at the Laboratory of Hydraulic Constructions revealed that these pool bottom pressure fluctuations may be amplified inside underlying rock joints and are directly responsible for progressive break-up of the rock.

Hence, appropriate assessment of these pressure fluctuations is crucial for a physically correct scour evaluation. At present, a respective amount of data is available on dynamic pressure fluctuations measured on laboratory models and for perfectly flat pool bottoms. However, real-life plunge pools are characterized by a much more complicated bottom profile. The simplest observable shape of a real-life bottom profile is not flat but rather triangular or elliptical.

Therefore, a research project has been elaborated focusing on measurements of dynamic pressure fluctuations at appropriately shaped, laboratory scaled pool bottoms. The bottom profiles to be tested have been derived from an extensive literature review of observed model and/or prototype cases. The obtained results will be systematically analyzed and compared with similar results but for flat pool bottoms. The first results are described in a companion paper by Manso et al. (2004).

This approach will allow assessing the influence of the plunge pool bottom geometry on the process of progressive break-up of fractured rock.

2 EXPERIMENTAL FACILITY

2.1 *General*

The experimental set-up (Fig. 1) consists of two main parts (Bollaert, 2002): a) a 3 m diameter cylindrical basin in steel reinforced plastic, simulating the plunge pool, and b) a 1 mm thin steel sheeting, modeling the rock joint. This steel sheeting is pre-stressed between two 100 mm thick steel plates with a weight of 1 ton each. The jet outlet has a cylindrical or convergent shape, for a nozzle diameter of 0.057 m or 0.072 m. The installation produces mean jet velocities of maximum 35 m/s. A series of maximum 8 flush-mounted micro pressure sensors (pressure range 0-17 bar, 3 mm diameter diaphragm) simultaneously record dynamic pressure fluctuations at the plunge pool bottom and inside the rock joint, for data acquisition rates of 1-20 kHz. The water depth in the plunge pool can be varied from 0 to 0.9 m. This is sufficient to create a high-velocity diffusing turbulent shear layer that impacts the underlying rock joint.

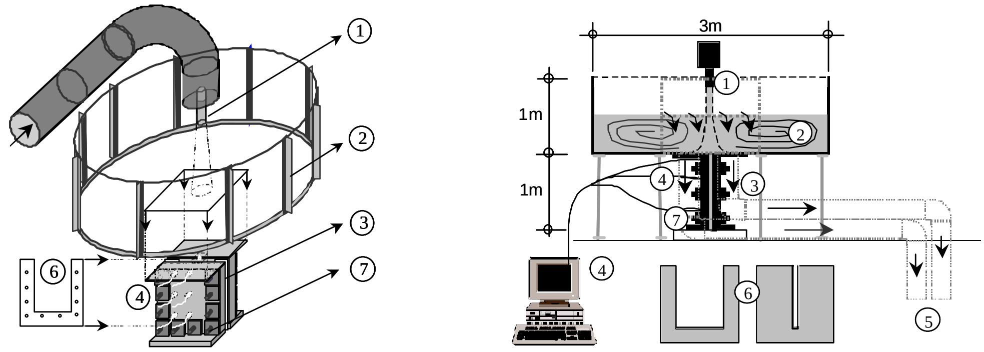

Figure 1. Perspective view and side view of the experimental facility: 1) cylindrical jet outlet, 2) reinforced plastic cylindrical basin, 3) pre-stressed two-plate steel structure, 4) Pressure sensors, 5) restitution system, 6) thin steel sheeting pre-stressed between steel structure (defining the form of artificial 1D-2D joints), 7) pre-stressed steel bars.

The turbulence intensities at the jet outlet have been measured between 3 and 6 %. The observed jets are compact because of their small fall heights (max. 0.50 m) and a small degree of break-up (max. 0.35).

2.2 *Turbulence conditions in pool*

The impact of a jet into a pool is governed by jet diffusion through a medium at rest. Momentum exchange with the pool creates a progressively growing shear layer, characterized by an increase of the jet's total cross section and a convergence of the core of the jet (Fig. 4). Dynamic pressures acting at the water-rock interface can be generated by core jet impact, occurring for small plunge pool depths, or by impact of a fully developed macroturbulent shear layer, occurring for ratios of pool depth to jet thickness Y/Dj higher than 4 to 6. The exact Y/Dj ratio dividing these two regimes depends on jet outlet conditions and low-frequency jet stability. For the present study, a value of Y/Dj between 5 and 6 has been deduced from the tests.

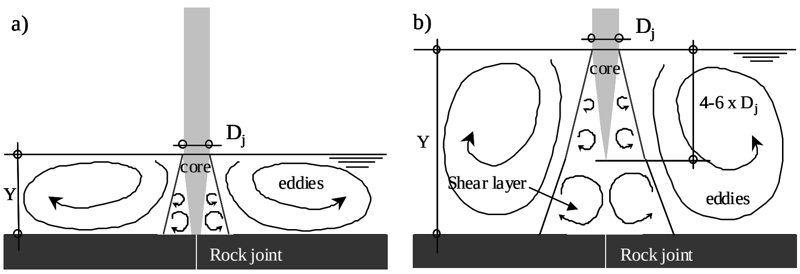

Figure 2. Plunging jets: a) jet core impact (for Y/Dj < 4-6); b) developed jet impact (for Y/Dj > 4-6)

3 DYNAMIC PRESSURES AT FLAT POOL BOTTOMS

3.1 *Mean and fluctuating dynamic pressures*

The mean and root-mean-square dynamic pressure values are defined at the jet's centerline (subscript a). The mean pressure measurements are presented in Figure 3a for core and developed jet impact conditions. The mean dynamic pressure coefficient C_{pa}, defined as the mean dynamic head divided by the kinetic energy of the impacting jet

$$C_{pa} = \frac{\dfrac{p^{mean}}{\gamma}}{\dfrac{V^2}{2g}} \tag{1}$$

shows similar tendencies with the best fits of available literature data on circular impinging jets (Franzetti & Tanda, 1987; Ervine et al., 1997). However considerable scatter can be observed for all jet impact conditions. The scatter is due to variability in the aeration rate and jet turbulence. Ervine et al. (1997) defined C_{pa} as a function of Y/D_j and of the air concentration α_i, at the impact point in the pool:

$$C_{pa} = 38.4 \cdot (1-\alpha_i) \cdot \left(\frac{D_j}{Y}\right)^2 \qquad \text{for } Y/D_j > 4\text{-}6 \tag{2}$$

$$C_{pa} = 0.85 \qquad \text{for } Y/D_j < 4\text{-}6$$

The air concentration at impact α_i is defined as a function of the volumetric air-to-water ratio β:

$$\alpha_i = \frac{\beta}{1+\beta} \tag{3}$$

A summary of expressions for β can be found in Bollaert (2002). As shown in equation (3), the mean dynamic pressure decreases with increasing air content in the plunge pool. This, however, does not take into account the jet turbulence. Jet turbulence can have a significant influence on the mean pressure value. In the present facility, the higher mean values of C_{pa} were obtained at very high air concentrations with a jet having a low turbulence level.

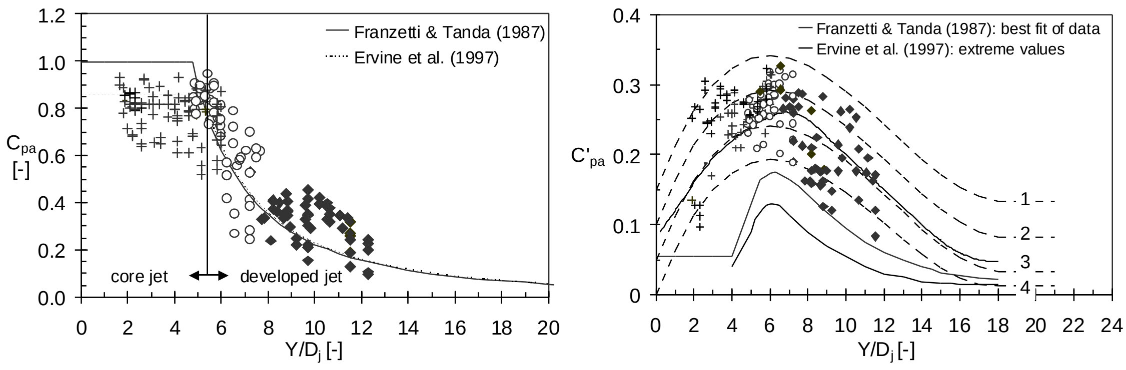

Figure 3. a) Non-dimensional mean dynamic pressure coefficient C_{pa} as a function of Y/D_j; b) Non-dimensional fluctuating dynamic pressure coefficient C'_{pa} as a function of Y/D_j.

The root-mean-square pressure coefficient C'_{pa} of the fluctuating part of the dynamic pressures is presented in Figure 3b and is defined as the root-mean-square value of the fluctuating dynamic head (RMS) divided by the kinetic energy of the impacting jet

$$C'_{pa} = \frac{\frac{RMS}{\gamma}}{\frac{V^2}{2g}} \tag{4}$$

The general form of the relationship between the root-mean-square values and the Y/D_j ratio is in good agreement with previous findings and with the theory of two-dimensional diffusion of a jet through a medium at rest. Initially, turbulence increases with increasing plunge pool depth until a certain maximum value is obtained. Then it decreases again with further increasing plunge pool depth due to increasing diffusion effects.

The data are significantly higher than previously reported values (Ervine et al. (1997) and Franzetti & Tanda (1987)). The mean increase of C'_{pa} is on the order of 0.05 to 0.10. This is not surprising when one considers that the facility generates near-prototype spectral characteristics. As pointed out before, the higher frequency part of the spectral content of an impacting jet is much closer to reality than on small-scale models. The root-mean-square values are obtained by integration of the spectral curves over the frequency range of interest and, thus significantly higher values are obtained.

For core jets, large scatter is obtained, with values ranging between 0.10 and 0.35. The lower values correspond to ideal core jet impact conditions, i.e. without any jet instabilities. For these impact conditions and for small jet fall lengths, the turbulence of the jet at the pool bottom becomes very close to the initial jet turbulence intensity Tu. The latter was estimated at the present facility at 0.04 to 0.05. Similar results were obtained by Franzetti & Tanda (1987), who apparently only considered perfect core jet impact conditions.

No ideal core jet impact is observed on the present facility. Apparently, even a small water depth is able to destabilize the core of the impacting jet such that its fluctuations at impact are substantially higher than the initial turbulence intensity Tu. Similar results have been obtained by most of previous research and are obviously not that unusual. For example, Ervine et al. (1997) seem to have encountered the same effects. Their values for core jet impact lie between 0.03 and 0.22, which indicates the results might have been influenced by core instabilities. This phenomenon has, to the authors' knowledge, never been investigated.

For developed jet impact, maximum values of C'_{pa} of up to 0.30-0.35 are obtained, for Y/D_j ratios between 5 and 8. Although diffusion effects become predominant at higher ratios, resulting in a quasi-linear decay of the root-mean-square values, substantial high values (0.25) may still persist at Y/D_j ratios of up to 10-11.

The measured data points have been approximated by a third order polynomial regression (equation (7)). This polynomial form has been obtained through curve fitting the upper limit of the data as given by Ervine et al. (Figure 3b). The regression coefficient for this curve fitting was equal to 0.99 and yielded the following relationship:

$$C'_{pa} = a_1 \cdot \left(\frac{Y}{D_j}\right)^3 + a_2 \cdot \left(\frac{Y}{D_j}\right)^2 + a_3 \cdot \left(\frac{Y}{D_j}\right) + a_4 \tag{5}$$

The coefficients a_1 to a_4 are summarized in Table 1 and define four similar-shaped curves but with different offsets. These curves agree with the measured data and can be used up to a Y/D_j ratio of 18-20. For higher ratios, the value that corresponds to a ratio of 18-20 are proposed. The offset depends on the initial turbulence intensity Tu of the jet.

Table 1 Polynomial coefficients and regression coefficient for different turbulence intensities.

Tu [%]	a_1	a_2	a_3	a_4	Type of jet
< 1	0.000220	-0.0079	0.0716	0	compact
1-3	0.000215	-0.0079	0.0716	0.050	intermediate
3-5	0.000215	-0.0079	0.0716	0.100	undulating
> 5	0.000215	-0.0079	0.0716	0.150	very undulating

The curve with the highest root-mean-square values is valid for jets with an undulating character or jets with a Tu that is higher than 5 %. The curve with the lowest values is applicable to a turbulence intensity that is lower than or equal to 1 %. In between, two other curves have been defined. They are appropriate for intermediate turbulence levels.

The key issue is that the low-frequency pressure fluctuations have been directly related to the turbulence intensity, Tu. This was defined as the root-mean-square value of the longitudinal velocity. In fact, the turbulence intensity comprises a whole range of frequencies each of which will influence the pressure fluctuation. Nevertheless, it is believed that the turbulence intensity defined by Tu can be used as the significant parameter.

Based on the experimental results, it is recommended to relate the choice of C_{pa} to the choice of C'_{pa} in the following manner: the higher the selected curve of root-mean-square values, the lower the choice for the mean pressure value. This is logical when considering that turbulent jets generate high root-mean-square values, but low mean pressures.

3.2 *Extreme dynamic pressures*

The extreme positive and negative pressure coefficients C_{pa}^{+} and C_{pa}^{-} are presented in Figure 4. They are defined as the net positive and negative fluctuation from the mean dynamic pressure value divided by the kinetic energy of the jet:

$$C_{pa}^{+} = \frac{\dfrac{p^{max} - p^{mean}}{\gamma}}{\dfrac{V^2}{2g}} \qquad (6) \qquad\qquad C_{pa}^{-} = \frac{\dfrac{p^{mean} - p^{min}}{\gamma}}{\dfrac{V^2}{2g}} \qquad (7)$$

The trend of data is in good agreement with available literature data, while the absolute values are far more extreme. For positive extremes, the measured C^{+}_{pa} values are higher by a value of 0.10-0.50. For negative extremes, the differences in C^{-}_{pa} values range from 0.10 to 0.30. Extreme values obtained at submerged jet outlet conditions are in better agreement with previously published data although the negative extremes are larger.

It is believed that the larger extreme values are again the result of the use of near-prototype jet velocities. Another reason could be the high air entrainment because extreme values that were obtained under submerged jet conditions (without any air) are in good agreement with previous data.

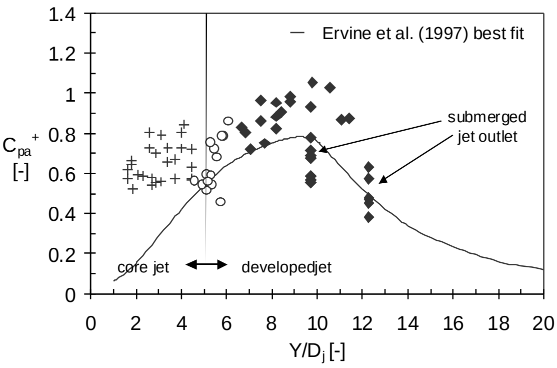

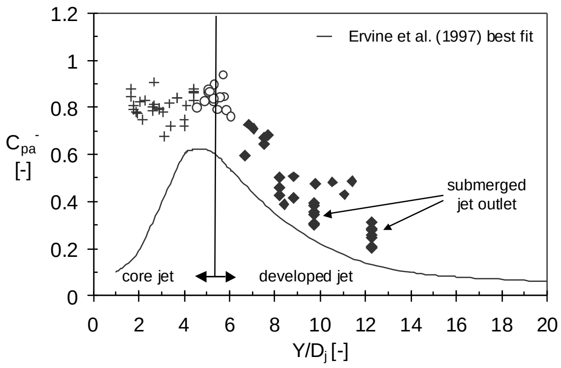

Figure 4. a) Non-dimensional positive extreme dynamic pressure value C_{pa}^{+} as a function of the ratio Y/D_j; b) Non-dimensional negative extreme dynamic pressure value C_{pa}^{-} as a function of the ratio Y/D_j

3.3 *Spectral energy of dynamic pressures*

The spectral content of the pressures under the jet's centreline S_{xx} is analyzed in the frequency and the Strouhal domain. $S_{xx}(f)$ is defined as a decomposition with frequency of the variance σ^2 of the pressure fluctuations. It is presented in non-dimensional form by dividing it by this variance. The spectral content defines the cyclic character of the pressures and indicates how the energy of the jet is distributed over different frequencies. The Strouhal number $S_{h,p}$ is defined as follows:

$$S_{h,p} = \frac{f \cdot Y}{V_j} \tag{8}$$

in which f stands for the frequency (in [Hz]) and V_j for the mean jet velocity at impact in the plunge pool (in [m/s]). The eddies of the shear layer are governed by Y and V_j. Hence, dynamic pressures at the pool bottom that directly result from these eddies should also depend on these parameters. Moreover, the non-dimensional spectral contents in the Strouhal domain should be similar for different jet velocities. Dynamic pressures measured outside of the shear layer do not follow this law. They depend on Y but the governing velocity field is completely different. Figure 5 shows the non-dimensional power spectral density corresponding to a 72 mm jet diameter. The results are presented for core jets and developed jets and for the frequency and Strouhal domains. Figure 5a shows that the spectral curves for core jet impact are characterized by a linear decay with a slope of -1, even at high frequencies (beyond 100 Hz). Moreover, it can be seen by Figs. 5a & 5b that core jet impact does not collapse to a single curve in the non-dimensional domain. The spectral curves collapse to a single curve in the frequency domain because the surrounding turbulent shear layer and related eddy sizes do not affect the core of the jet. On the other hand, developed jet impact produces more spectral energy at low and intermediate frequencies as shown in figures 5c and 5d. The spectral curves decay at a quasi-linear –7/3 slope, corresponding to values available in literature (Bearman, 1972; Huot et al., 1986).

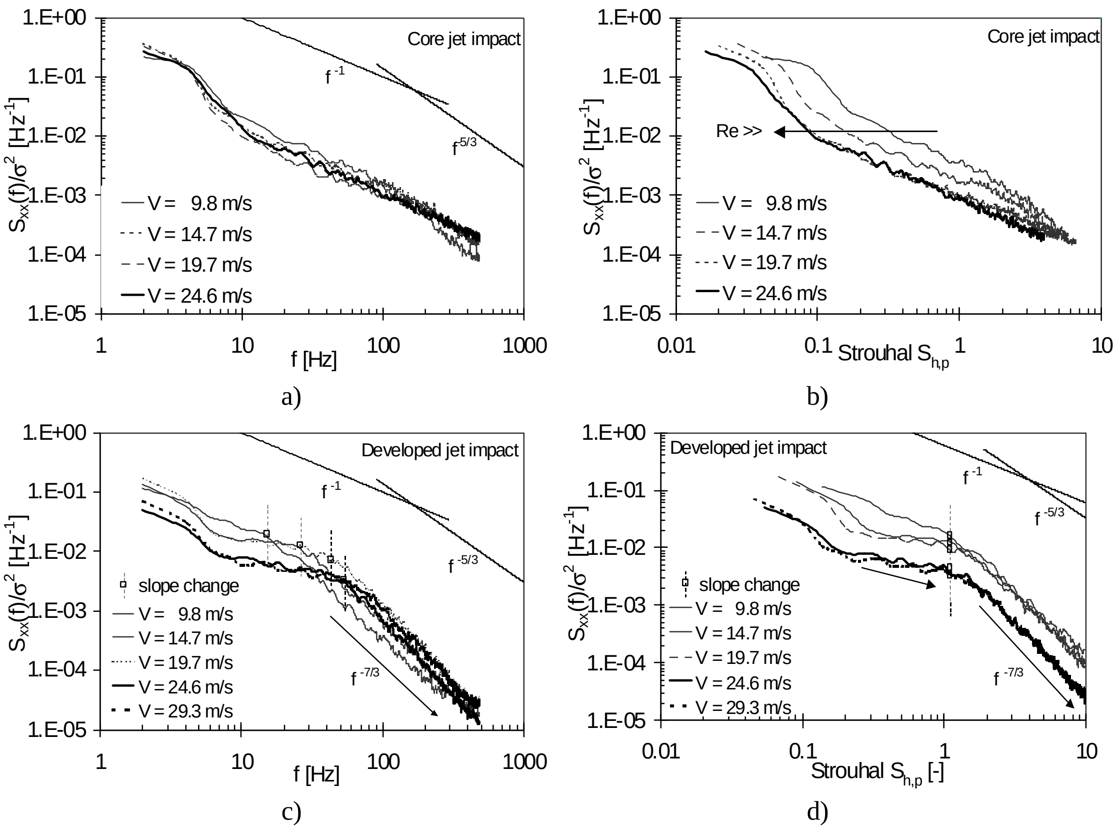

Figure 5. Non-dimensional power spectral density of dynamic pressures at the plunge pool bottom: a) core jet in the frequency domain; b) core jet in the Strouhal domain; c) developed jet in the frequency domain; d) developed jet in the Strouhal domain.

4 REAL-LIFE POOL BOTTOM CONFIGURATIONS

The aim of the research project is to measure pressure fluctuations inside more realistic plunge pool and rock joint geometries. Previous tests were performed for a cylindrical plunge pool with a perfectly flat bottom. This, however, only happens in the beginning of the erosion process; with progressing scour of the rock mass, the form of the pool bottom transforms into a highly irregular shape (Kobus et al., 1979; Rajaratnam, 1981). This shape is thereby influenced by the joint sets and the relative strength of the rock mass. Some possible shapes are presented in Figure 6.

The first shape is conical (Fig. 6a), with slope angles close to the natural angle of repose of the fractured rock material. This shape corresponds to the ones generally observed on granular bottoms and is representative for highly fractured rock or rock with a very low erosion resistance. The corresponding sketch presents the possible parameters of such a pool bottom, i.e. the height and the width of the steps, as well as the angle of the average slope of the pool walls.

The second shape (Fig. 6b) is typical for rock with a high degree of fracturing in the horizontal direction and a high erosion resistance. This automatically results in deep scour holes with slope angles that are much steeper than the natural angle of repose of the material. Such a particular (cylindrical) shape might have a profound influence on the diffusion and recirculation pattern of the jet in the pool.

The last shape is asymmetrical and considers a rock mass that is highly jointed in one particular direction. This conducts to a skewed V-shape as presented (Fig. 6c). The corresponding sketch indicates how the experimental facility accounts for this shape. As the angle of impact of the impacting jet is fixed, the rock mass has been rotated to match with the jet and to respect the relative angles between the jet and the slope of the walls.

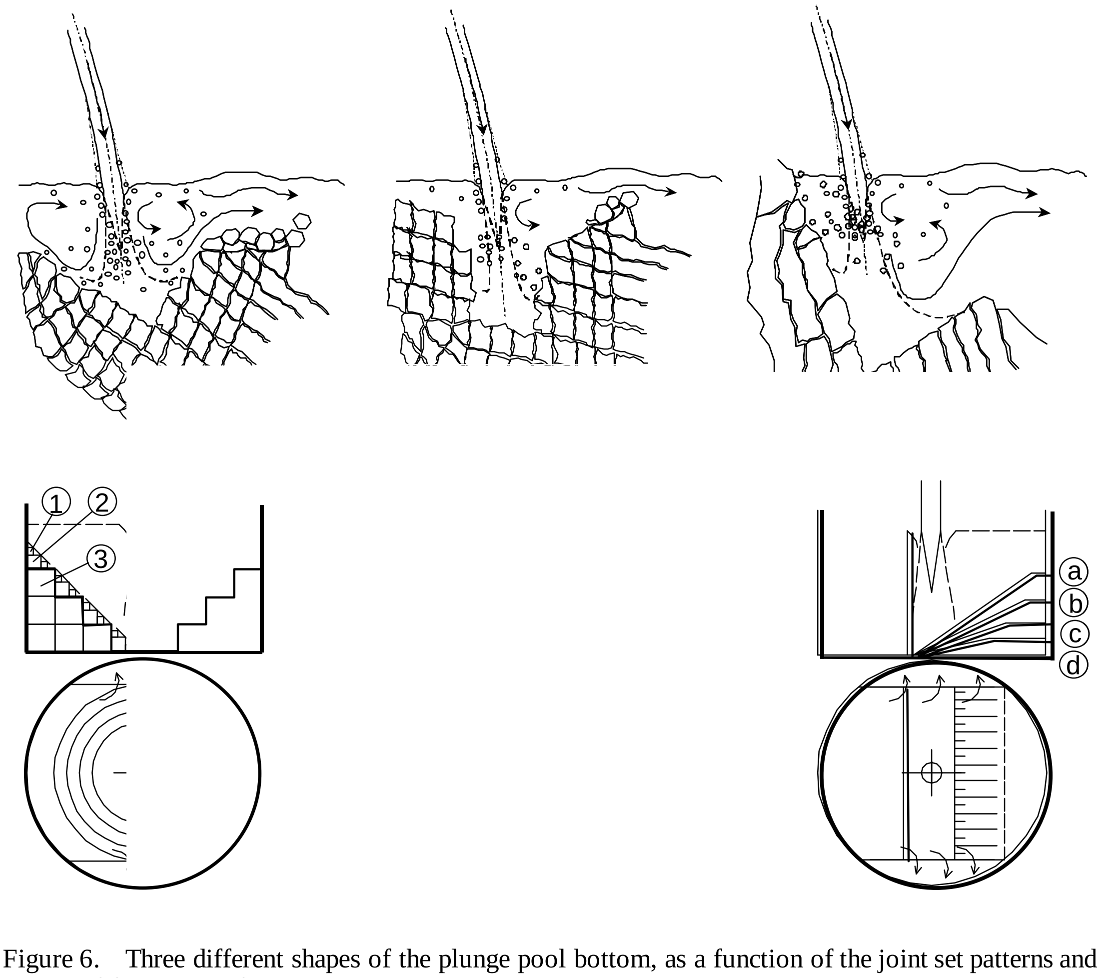

Figure 6. Three different shapes of the plunge pool bottom, as a function of the joint set patterns and the degree of fracturing of the rock mass: a) conical shape with varied roughness (1, 2, 3), b) cylindrical shape with varied diameter, c) skewed V-shape with varied slope (a, b, c, d).

The recirculating eddies of the turbulent two-phase shear layer of the impacting jet are influenced by the shape of the pool bottom. As such, the spatial distribution of the pressure fluctuations at the pool bottom should be quantified for different bottom configurations. In addition, the statistical characteristics of the hydrodynamic flow should be assessed for the corresponding integral scales of turbulence and persistence time of maximum pressures. This should allow to define to which extend the turbulent fluctuations of the jet change during the scouring process and the ability of the corresponding vorticity to up-lift potential rock blocks

5 CONCLUSIONS

The present article presents the results of near-prototype scaled measurements of dynamic pressure fluctuations at flat plunge pool bottoms. Statistical characteristics of the dynamic pressures are analyzed in both the time and the frequency domain, and a comparison with available scaled literature data is made.

Furthermore, the basis for new dynamic pressure investigations are outlined, focusing on the assessment of the mutual influence of the plunge pool bottom geometry and the development of dynamic pressure fluctuations. This aspect is of direct relevance to scour hole formation and is discussed in a companion paper by Manso et al. (2004).

REFERENCES

Bearman, P.W. 1972. An investigation of the forces on flat plates normal to a turbulent flow. *Journal of Fluid* Mechanics. (46) 177-198.

Bollaert, E. 2002. Transient water pressures in joints and formation of rock scour due to high-velocity jet impact. *Communication 13 Laboratory of Hydraulic Constructions*. EPFL. Switzerland.

Bollaert, E., Falvey, H.T. & Schleiss, A. 2002. Assessment of turbulent jet impingement in plunge pools: the particular characteristics of a near-prototype physical model study. *Proceedings of Riverflow 2002*. Louvain-la-Neuve. Belgique.

Ervine, D.A., Falvey, H.R. & Withers, W. 1997. Pressure fluctuations on plunge pool floors. *Journal of Hydraulic Research*, IAHR. (35) 2.

Franzetti, S. & Tanda, M.G. 1987. Analysis of turbulent pressure fluctuation caused by a circular impinging jet. *International Symposium on New Technology in Model Testing in Hydraulic Research*. India: 85-91.

Manso, P.A., Bollaert, E.F.R, Schleiss, A.J., 2004. Experimental investigations on jet behaviour in plunge pool rock scour. International Conference on Hydraulics of Dams and River Structures, Teheran, Iran

Kobus, H.; Leister, P. & Westrich, B. 1979. Flow field and scouring effects of steady and pulsating jets impinging on a moveable bed. *Journal of Hydraulic Research*. (17) 3: 175-192.

Rajaratnam, N. 1981. Erosion by plane water jets. *Journal of Hydraulic Research*. (19) 4: 339-358.

Huot, J.P.; Rey, C. & Arbey, H. 1986. Experimental analysis of the pressure field induced on a square cylinder by a turbulent flow. *Journal of Fluid Mechanics*. (162): 283-298.